A Fast and Accurate Method for Automatic Segmentation of Colons at CT Colonography based on Colon Geometrical Features

Tarik A. Chowdhury
Centre for Image Processing & Analysis
School of Electronic Engineering
Dublin City University
Dublin 9, Ireland
tarik@eeng.dcu.ie

Paul F. Whelan
Centre for Image Processing & Analysis
School of Electronic Engineering
Dublin City University
Dublin 9, Ireland
paul.whelan@dcu.ie

Abstract—**In CT colonography, the first major step of colonic polyp detection is reliable segmentation of colon from CT data. In this paper, we propose a fast and accurate method for automatic colon segmentation from CT data using colon geometrical features. After removal of the lung and surrounding air voxels from CT data, labeling is performed to generate candidate regions for Colon segmentation. The centroid of the data, derived from the labeled objects is used to analyze the colon geometry. Other notable features that are used for colon segmentation are volume/length measure and end points. The proposed method was validated using a total of 99 patient datasets. Collapsed colon surface detection was 99.59% with an average of 1.59% extra colonic surface inclusion. The proposed technique takes 16.29 second to segment the colon from an abdomen CT dataset.**

Keywords-component; CT colonography, colon segmentation, colon geometrical features, centroid.

I. INTRODUCTION

Computed Tomography (CT) colonography [1] is an alternative approach to colonoscopy for early detection of colonic polyp using CT data. Previous scientific studies show that the sensitivity of polyp detection for CT colonography (CTC) is comparable to colonoscopy [2-7]. The work flow of a complete automatic computer aided detection (CAD) system for CT colonography can be divided into four major steps: colon segmentation, polyp candidate generation, feature generation and classification. Hence, the sensitivity of polyp detection in CAD-CT colonography heavily relies on robust segmentation of colon from CT data. Currently, two types of bowel preparation are used in CTC. The first, involves bowel cleansing and inflation of colon with CO2 or room air prior to CT scan. The second method involves consumption of density enhancement fluid (barium contrast material or iodinated contrast material) and inflation of colon. Electronic cleansing is applied after colon segmentation for oral contrast patient data. Review of previous research work shows that automatic colonic surface detection techniques are proposed [8-21] for both kind of bowel prepared patient datasets. Our proposed method can be applied to both high contrast and without contrast patient data for colon segmentation.

Regarding existing techniques, Wyatt et al. [9] employed a distance transform of a binary data to extract the seed points. Detected seed points were applied for object labelling using 3D region growing algorithm. Wyatt et al. [9] employed an elongation criteria on the labelled objects for colon detection. Li et al. [16] applied a 2D region growing algorithm with automatic seed placement in each slice of the patient data. 2D regions were filtered using shape filters and size filters. In the last step, authors [16] employed filtered seed, a 3D region growing algorithm and elongation criteria for detection of the colon. Masutani et al. [17] proposed a method that identifiesthe largest air volume in the patient dataset as the colon (after removal of surrounding air voxels and lungs). If a collapse appears in the colon, the largest air volume in the patient data was assigned as the colon. The other air regions having volume 25% (Volume threshold R_{fc}) of the largest volume were considered as parts of the colon. Nappi et al. [18] proposed a different segmentation method that detects the colon as the intersection of Anatomy Based Extracted (ABE) surface with Colon Based Extracted (CBE) surface. ABE uses the same volumetric features proposed by Masutani et al.[17]. In the CBE method, a 3D region growing is initiated from the rectum and this process continues until a stopping rule that checks for certain experimentally validated conditions is upheld. If the conditions are not met, the region growing process is re-started from an automatically selected new seed point and the stopping rule is re-evaluated. Finally, the intersection surface between ABE and CBE is declared as the colon surface. This method reduced the extra-colonic surface inclusion from 25.6% to 12.6%. Iordanescu et al. [19] proposed an automatic seed placement method using one seed point near the rectum for well-distended colon and two seed points at rectum and cecum for collapsed colon segmentation. Their method shows 83.2% complete colon segmentation and 9.6% partial colon segmentation. The remaining 7.2% section of the colon requires a manual seeded segmentation. Frimmel et al. [20] proposed a method that uses the centerline and the

colon geometry for automatic segmentation. They [20] calculated the bounding box parameters for each centerline and used some predefined thresholds to accept or reject the centerline section derived from the small intestine. Their method shows 96% sensitivity for automatic colon segmentation. In our previous method [21] volume/length analysis, distance between the labeled objects, and gradient of centerline were used as geometrical features for colon detection. Our previously developed method showed 96.52% sensitivity for colon segmentation with 99% colonic surface area detection. The new proposed method uses centroid based geometry analysis of the air inflated region inside the CT data for colon segmentation. The proposed method is fast and robust for detection of colon compare to our previously developed method reported in [21].

II. Automated Segmentation of Colon

Automatic colon segmentation from abdomen CT data starts with surrounding air voxel removal and lung detection. The next step identifies and labels all remaining air regions in the volumetric data and calculates the centroid of the patient data. The colon is declared well distended or collapsed by the analysis of centroid based colon geometry. Fig. 1 illustrates the four main steps required for colon segmentation from CT data.

Patients can be scanned head first supine/prone or feet first supine/prone in a CT scan. If the patient is scanned in feet first supine/prone, data is rotated 180 degrees around the Z-axis to make it head first supine/prone. Hence, in all volumetric CT data the lungs are always visible in the first slice. Consequently, after removal of the surrounding air voxels, 3D region growing starting in the first slice of the volumetric data will segment the lung regions. To detect the lungs, the proposed algorithm checks for the presence of isolated blood vessels inside the segmented area. If multiple isolated blood vessels / pulmonary vessels are detected, the segmented area is defined to be lung; otherwise it is defined to be a candidate region for the colon structure [21].

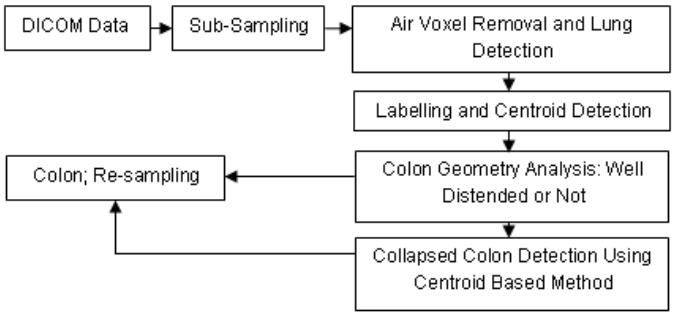

Figure 1: Overview of colon segmentation in CAD-CTC.

A. *Labelling the Inside Area*

Once the lungs have been segmented, the remaining air regions represent colon, small intestine, a few external objects and stomach. In the next step, labelling is performed using a 26-neighbourhood region growing algorithm [22]. The threshold for region growing is automatically selected from the global histogram [21] and is usually in the range -900HU to -800HU. The labelling of the air regions is performed in two phases. In the first phase, any air voxels (less than the threshold) in the volumetric data initiate the region growing and continue to label all the connected air voxels. The region growing process stops when no neighbouring voxel with HU value less than the threshold is found. The last voxel where the region growing stops is considered as the first end point (FEP) (see Fig. 2a) of that labelled region. In the second phase, region growing starts from the first end point and labels all the voxels in the region that are already checked in the first phase of labelling. We also store the (X,Y,Z) coordinates of voxels that are in 10mm incremental (10mm, 20mm …) distance from the first end point. The 2D projection of the stored (X,Y,Z) points are also calculated in the X-Z plane (see Fig. 3). Let (X_{10i},Z_{10i}) be the projected coordinates of 10mm distance voxels starting from the first end point. Equation 1 is employed to calculate the final (X_{10},Z_{10}) for 10mm points. Similarly, all 10mm incremental points (X_i,Z_i) are calculated using equation 1. Let M be the number of labelled objects inside the patient data and let (X_{Mi},Z_{Mi}) be the points that are at 10mm incremental distances for each labeled object. The centroid (X_c,Z_c) of the dataset is derived from each of the labelled objects points (X_{Mi},Z_{Mi}) using equation 2. Fig. 4 shows the centroid of patient data that is calculated from the labeled objects points (X_{Mi},Z_{Mi}). At the end of the second phase, the last voxel where the region growing stops is considered as the second end point (SEP) (see Fig. 2b). During the labelling process the following information is also stored for each labelled region: total voxel count, labeled volume, and Euclidian distance between the two end points.

$$(X,Z) = \frac{1}{n}\sum_{i=1}^{n}(X_i,Z_i) \quad (1)$$

where n is number of points at a certain distance.

$$(X_c,Z_c) = \frac{1}{MN}\sum_{i=1}^{M}\sum_{j=1}^{N}(X_{Mi},Z_{Mi}) \quad (2)$$

where M is number of labelled objects in the dataset and N is number of 10mm incremental points in each labelled object.

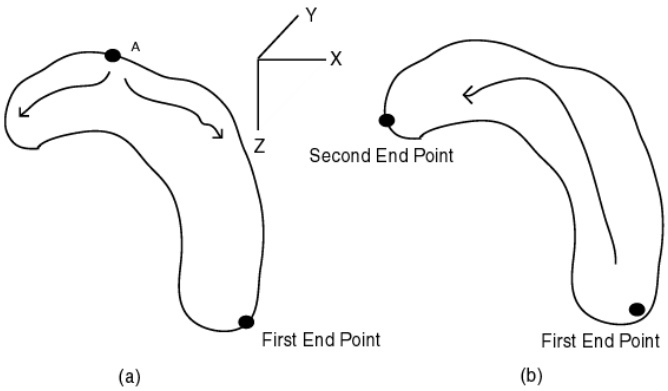

Figure 2: Labelling the patient CT data using seeded 3D region growing algorithm. (a) shows the detection of first end point and (b) shows the detection of second end point.

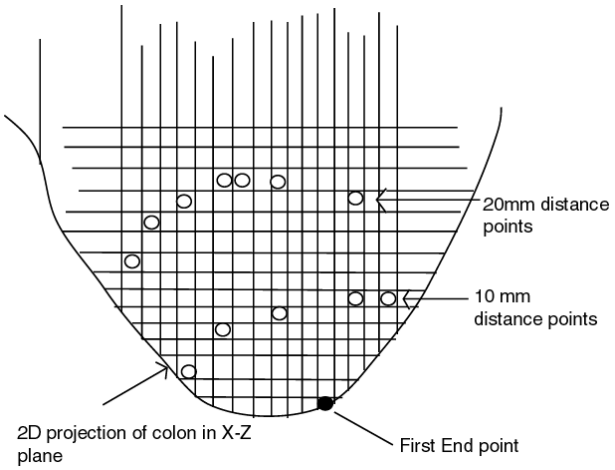

Figure 3: 10mm incremental distance points from the first end point.

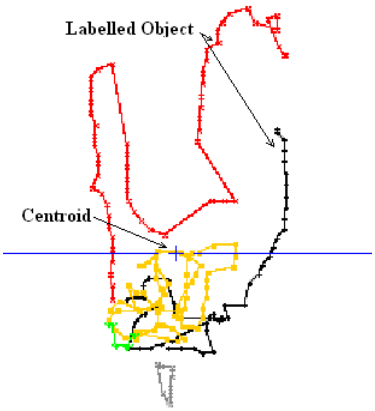

Figure 4: Centroid and 2D projected points (X_{Mi},Z_{Mi}) of all the labelled objects inside a patient dataset.

B. Colon Detection

The adult colon and small intestine are approximately 1.5m and 7-10m long respectively [23]. Anatomy of the colon shows that it is shorter and thicker than the small intestine. In our previous method [21], we employed volume by length (*V/L*) analysis to differentiate colon from small intestine. In our new method, geometry of the colon is measured with respect to the centroid of patient data.

The devised algorithm firstly checks whether the colon has a collapsed segment or not. Fig. 5a illustrates a well distended colon and 5b shows the centroid of the dataset with well distended colon in it. The algorithm is initiated with the detection of the rectum. In general, the rectum is the only air filled area that is located at the lower end of the dataset. If multiple objects are selected as candidate rectum points, the object with the highest *V/L* is selected as the rectum. The colon will be declared as intact if the selected rectum object fulfills four conditions:

i) *if length* of labelled *object > 700mm*
ii) *if V/L* is greater than *300mm*^{2}
iii) *loop i = 1,... n* [where n is the number of points on a labelled object]
if Z_{Mi} is less than centroid $_{Zc}$ [where M is the number of labelled objects in the patient data]
$Angle_{Li}$ = (X_{Mi},Z_{Mi}) with X-axis of the centroid (X_c,Z_c)
if $Angle_{Mi}$ is less than *min_angle*
min_angle = $Angle_{Mi}$
end if
if $Angle_{Li}$ is greater than *max_angle*
max_angle = $Angle_{Li}$
end if
end if
end of loop
if min_angle is less than 10 degrees and *max_angle* is greater than 170 degrees
coverage_area = **true**;
else
coverage_area = **false**;
end if
iv) *The proposed algorithm also checks in the cecum area for any disconnected region having a V/L value greater than 500mm*^{3}*. If such a region is found in the ascending colon/cecum area, the colon is declared as collapsed.*

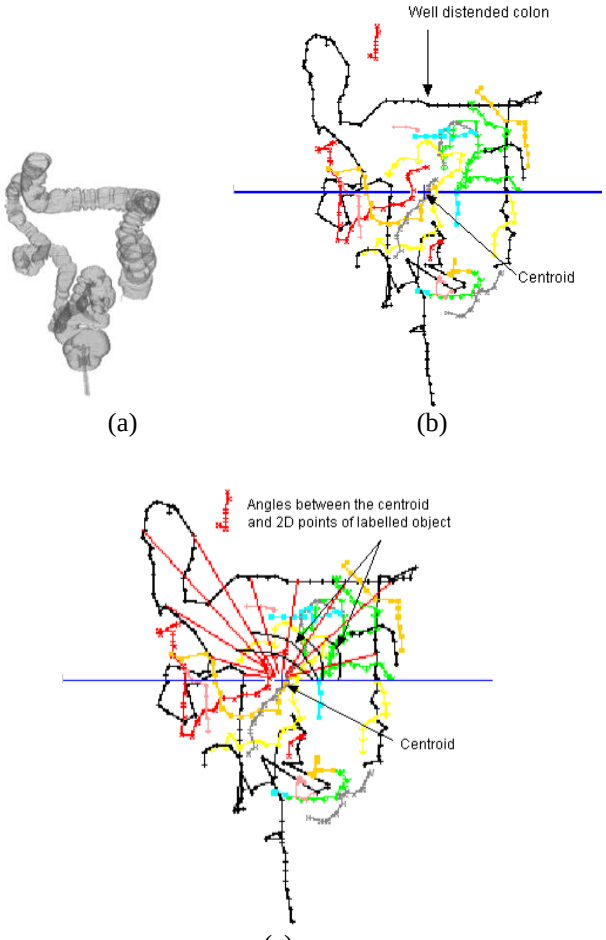

Figure 5: Well distended colon detection. (a) shows the 3D surface of a well distended colon, (b) illustrates the centroid and all the labelled objects inside a patient dataset, (c) shows the calculation of coverage area for a candidate labelled object.

It is worth noting that the length of a large intestine is above *1400mm*. The threshold in the first condition (*i*) is set *700mm* to justify that the length of detected rectum object must be greater than half of the length of a standard colon. The second condition (*ii*) is set empirically after analyzing *V/L* ratios [21] of 35 patients data. The algorithm presented in the third condition (*iii*) is applied to analyze the coverage area of the colon with respect to the centroid. For supine/prone view a coverage area of 170 degrees means the rectum object includes the descending colon, the transverse colon and part of the ascending colon (see Fig. 5c). Finally, condition (*iv*) is employed to identify collapsed colon segments in the ascending colon/cecum (see Fig. 6). If the detected rectum object passes all the above mentioned conditions (*i-iv*), we declare the colon as well distended.

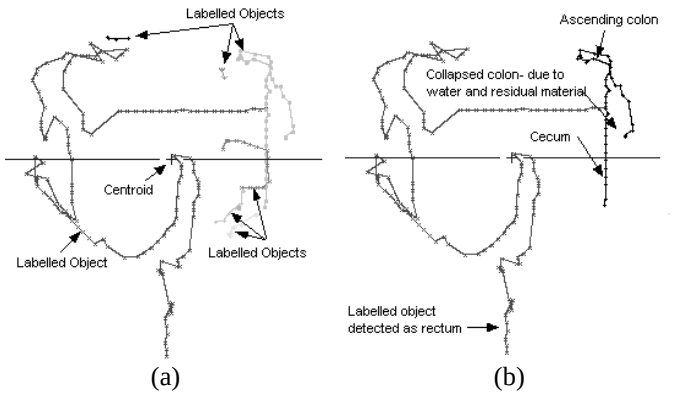

Figure 6: Collapsed colon detection. (a) shows all the labelled objects in the patient dataset and (b) detected collapsed segment in the cecum area.

In the case of a colon being flagged as well distended, the single region including the rectum point represents the complete colon as segmented, and the colon detection procedure is complete. Otherwise we proceed as follows. Collapsed colon detection also starts from the detected rectum point. It detects the closest placed large segments ($V/L > 300mm^2$) using the Euclidean distance between the end points (see Fig. 7) and the algorithm checks for condition (iii) detailed above. This process is iterated until this condition is upheld (see Fig. 7). Fig. 7 shows five colon segments (*L1*,*L2*, *... L5*) that are detected during the iterative process of large segment detection. The remaining small air filled regions (with $V/L < 300mm^2$) are either part of the small intestine or part of the colon. As their anatomical and geometrical properties are quite similar, perfect colon identification is far from a trivial task. Our proposed segmentation scheme analyses the small segments using their geometrical position between the large segments (such as *L1,…,L5* in Fig. 7) with respect to the centroid (X_c,Z_c). The geometrical position of small region is verified using length, Euclidian distance and orientation. Orientation of a small object is calculated using its' angular position with respect to the centroid (X_c,Z_c) of the patient data. The method of small colon segment detection is an iterative process. In the first iteration, the proposed algorithm detects the small objects that are found between the end points of the rectum (*L1*) and the next large segment (*L2*) (see Fig. 8a). A detected small object is considered as part of the colon if the orientation of the object is similar to the angle created by the end points of L1 and L2 (see Fig. 8a). The iterative process of small segment detection continues until all the large segments are checked (see Fig. 8b). Finally, the Fig. 8c illustrates the result of our automatic colon segmentation method for a patient data.

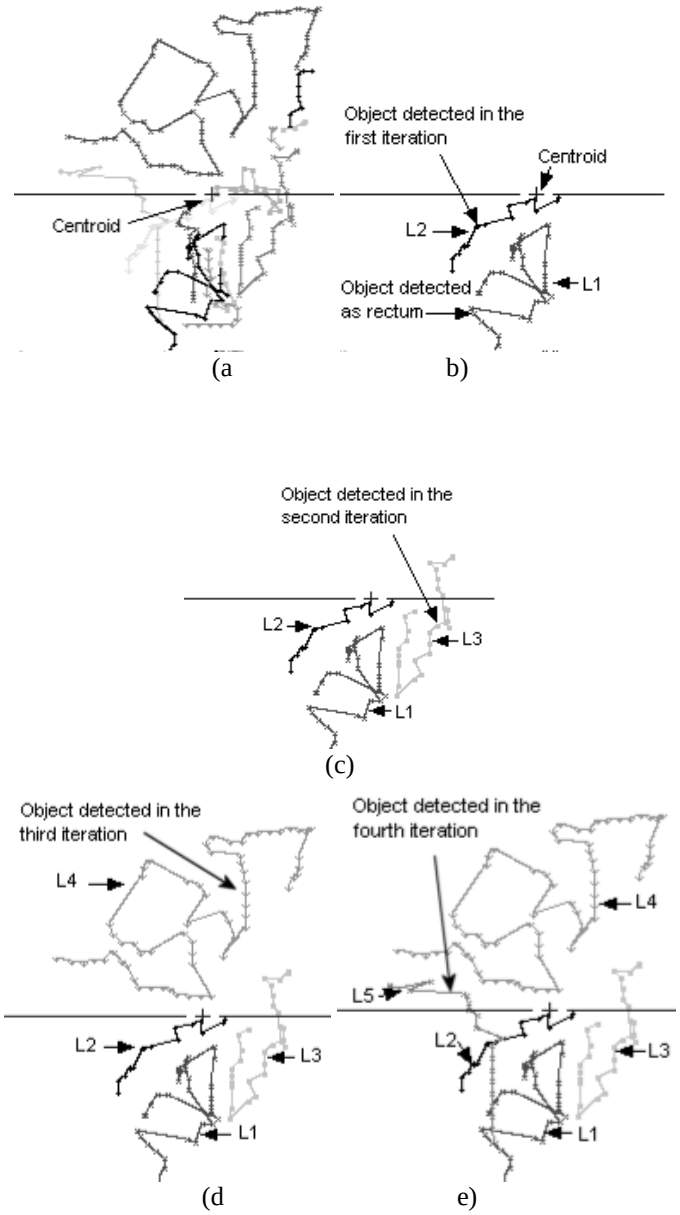

Figure 7: Large colon segment detection. (a) shows all the labeled objects inside the patient dataset. Process of large segment detection starts from the rectum. (b) - (e) demonstrate the iterative process that are applied for large segment detection.

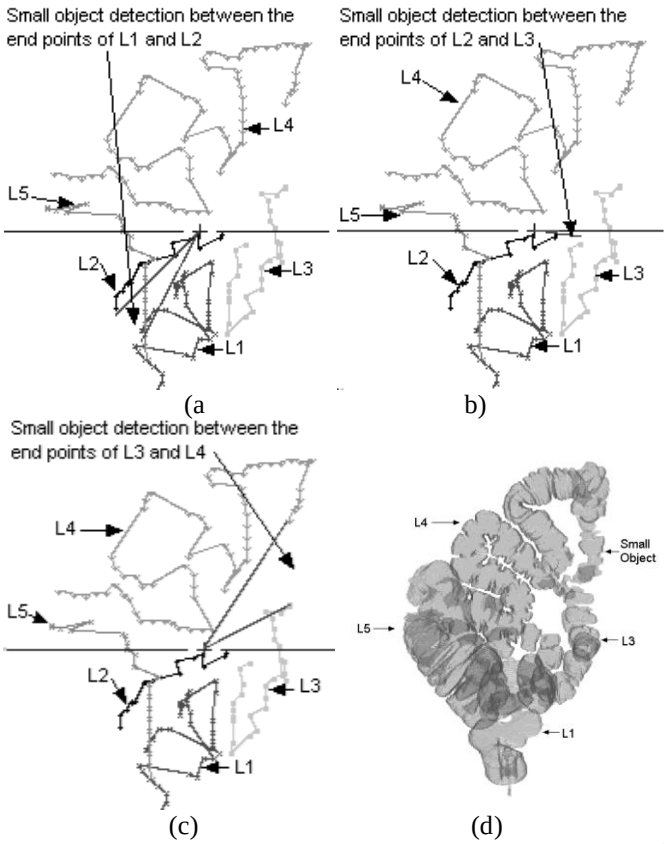

Figure 8: Small colon segments detection. (a)-(c) show the iterative process of small segment detection between the end points of L1 and L2, L2 and L3, L3 and L4 (d) illustrates the 3D surface of the segmented colon.

III. Results and Discussion

The developed algorithm was evaluated on 188 supine and prone standard and low-dose patient datasets (99 patients). All patients were scanned using the following CT protocol: 120kVp, 2.5x4mm/1.5x16mm collimation, 3mm slice thickness, 1.5mm reconstruction interval, and 0.5s gantry rotation. For standard (157 supine and prone) and low dose (31 supine and prone) data acquisition, patients were scans at 100mAs and 13-35mAs respectively. The scanning time ranged from 10s to 30s and the CT data acquisition was performed in a single breath-hold. The procedure was first performed with the patient with head first supine position and then repeated for the patient head first prone position. The number of slices per dataset varies from 200 to 350 depending on the height of the patient.

Our automatic segmentation method reliably detected 63 well-distended standard dose and 14 well-distended low dose colons without inclusion of any Extra Colonic Surface (ECS). Thus, the colon surface detection was 100% and the ECS error was 0% (Table 1). The method was applied to 94 standard dose and 17 low dose patient datasets with collapsed colon acquisitions. In the collapsed colons, average surface detection for standard dose datasets was 99.59% (Table 1). The largest ECS detection was 43.28% with a mean of 2.80%. Detection for collapsed colon was considered failed for 3 cases (out of 94 collapsed colons), as the surface detections were less than 95% with ECS surface inclusion higher than 15% (see Fig. 9 and Table 1). When the developed method was applied to 17 low-dose collapsed colons, the average surface detection was higher than 99.04%, with mean ECS inclusion of 1.50% (see Table 1). The average ECS inclusion for 188 supine and prone datasets (99 patients) was 1.59%.

Table 1: Results of automatic colon segmentation for well distended and collapsed colons

Number of patients	Dose	Colon surface (%)	Extra colonic surface inclusion (%)	Colon surface missing (%)
63 Well Distended	Standard	100	0	0
14 Well Distended	Low-Dose	100	0	0
91 Collapsed	Standard	99.59	2.80	0.409
17 Collapsed	Low-Dose	99.04	1.50	0.96
Patients 1 (failed)	Standard	82.12	9.64	17.88
Patients 2 (failed)	Standard	88.27	78.01	11.73
Patients 3 (failed)	Standard	97.93	80.01	2.07

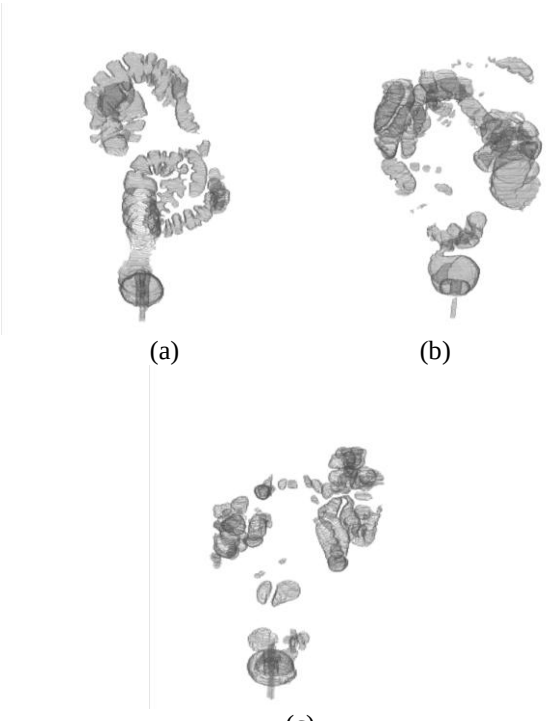

Figure 9: (a), (b) and (c) are 3D surface rendered views of patient 1, 2 and 3 (see Table 1) respectively.

To evaluate the performance of our automatic colon surface segmentations, two radiologists from Mater Misericordiae Hospital performed a manually seeded segmentation and we used their segmented data as ground truth data. The

radiologists segmented the colons manually using seed points and 3D region growing. Any area which was detected by the automatic colon segmentation algorithm but not found in the manually segmented data was declared as ECS (see Fig. 10). The performance of our algorithm compares well with the performance of other developed techniques (see Table 2). In this regard, the proposed methods' success rate (98.04%) is better than the method proposed by Frimmel et al. [20] (96%). The developed algorithm also outperforms other methods [9, 16-21] for detection of colonic surface (99.59%) and removal of ECS (1.59%). Another advantage of our technique is its low computational cost, where the typical processing time for overall segmentation is approximately 26.98 seconds (colon segmentation - 16.29 seconds, data interpolation - 10.69 seconds) on a 1.6 GHz Centrino Duo with 2GB RAM. The proposed method takes only 16.29 seconds to segment the entire colon from a subsampled patient dataset. The computation cost of our method (16.29 seconds) is similar to the method developed by Frimmel et al. [20] (14.8 seconds excluding data interpolation) where as the success rate of our method (98.04%) is better than the method developed by Frimmel et al. [20] (96%). The computation cost of our method also outperforms the methods reported in [9, 16-21].

TABLE 2: RESULTS OF DIFFERENT AUTOMATIC COLON SEGMENTATION METHOD IN CT COLONOGRAPHY

Method	**Number of patients**	**Time**	**Sensitivity (sen.) / Surface area detection (SAD)**	**Extra colonic surface inclusion (%)**
Wyatt et al. 2000	20	60 min	40 to 80% sen.	-
Li et al. 2005	50	6min	87.5%SAD	6.5
Napii et al. 2002	44	10 min	98%SAD	10-15
Frimmel et al. 2005	38	14.8 sec	96% sen. 99% specificity	-
Iordanescu et al. 2005	292	-	83.2% sen.	9.6 % requires manual intervention
Chowdhury et al. 2005	115 supine and prone	2-3min	96.52% sen. 99% SAD	1.07
Proposed method	99	16.29 sec	98.04% sen. 99.59% SAD	1.59

I. CONCLUSION

The developed method for automatic segmentation successfully identified the colonic lumen from volumetric CT data. In 188 supine and prone (99 patient datasets: 157 standard and 31 low-dose) datasets containing collapsed colon data, the segmentation method detected 99.59% of the colonic wall and shown 98.04% sensitivity for collapsed colon detection. The overall sensitivity of colon detection was 96.95%. In 63 datasets the well-distended colons were detected without any inclusion of extra-colonic surface. The performance of the developed algorithm makes it suitable for 3D visualization of the colon surface and for advanced polyp detection.

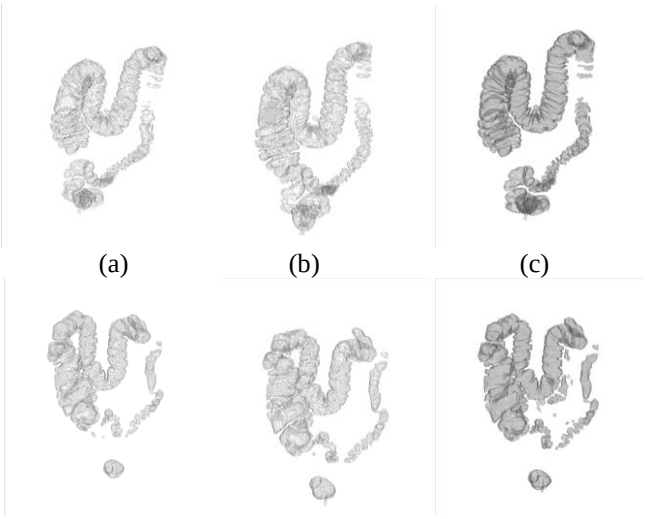

Figure 10: Comparison of automatic colon segmentation with manual segmentation by Radiologists. (a), (d) and (b), (e) illustrate the surfaces generated from manual segmentation of colon by Radiologists. (c) and (f) show the results of automatic segmentation of colon.

ACKNOWLEDGMENT

The authors would like to thank our medical collaborators Dr. Helen Fenlon, Dr. Alan O'Hare (Department of Radiology) and Dr. Padraic MacMathuna (Gastrointestinal Unit) at the Mater Misericordiae Hospital, Dublin. We would also like to acknowledge the valuable input from our colleagues from the Center for Image Processing & Analysis, namely, Robert Sadleir and Ovidiu Ghita. This work was funded by Rince Institute (DCU), National Biophotonics and Imaging Platform Ireland [NBIP] (HEA-PRTLI IV).

REFERENCES

[1] D.J. Vining, D.W. Gelfand, R.E. Bechtold. "Technical feasibility of colon imaging with helical CT and virtual reality," American Journal of Roentgenology, 162, 104, 1994.

[2] C.D. Johnson, A.K. Hara, J.E. Reed, "Virtual endoscopy: what's in a name?," American Journal of Roentgenology, 171, 1201-2, 1998.

[3] C.D. Johnson, M.H. Chen, A.Y. Toledano, J.P. Heiken, A. Dachman, M.D. Kuo, C.O. Menias, B. Siewert, J.I. Cheema, R.G. Obregon, J.L. Fidler, P. Zimmerman, K.M. Horton, K. Coakley, R.B. Iyer, A.K. Hara, R. A. Halvorsen, G. Casola, J. Yee, B.A. Herman, L.J. Burgart, and P.J. Limburg, "Accuracy of CT Colonography for Detection of Large Adenomas and Cancers," The New England Journal Medicine, 359(12):1207-1217, 2008.

[4] H.M. Fenlon, D.P. Nunes, P.C. Schroy, M.A. Barish, P.D. Clarke, and J.T. Ferrucci, "A comparision of virtual and convention colonoscopy for the 12 detection of colorectal polyps," The New England Journal Medicine, 341:1496-150, 1999.

[5] F.M. Vos, R.E. van Gelder, I.W. Serlie, J. Florie, C.Y. Nio, A.S. Glas, F.H. Post, R. Truyen, F.A. Gerritsen, and J. Stoker, "Three-dimensional

display modes for ct colonography: Conventional 3d virtual colonoscopy versus unfolded cube projection," Radiology, 228(3):878-85, 2003.

[6] S. Halligan, D.G. Altman, S.A. Taylor, S. Mallett, J.J. Deeks, C.I. Bartram, and W. Atkin, CT colonography in the detection of colorectal polyps and cancer: Systematic review, meta-analysis, and proposed minimum data set for study level reporting. Radiology, 237:893-904, 2005.

[7] P.J. Pickhardt, J.R. Choi, I. Hwang, J.A. Butler, M.L. Puckett, H.A. Hildebrandt, R.K. Wong, P.A. Nugent, P.A. Mysliwiec, and W.R. Schindler, "Computed tomographic virtual colonoscopy to screen for colorectal neoplasia in asymptomatic adults," The New England Jounal of Medicine, 349(23):2191-2200, 2003.

[8] M. Sato, S. Lakare, M. Wan, A. Kaufman, Z. Liang, and M. Wax, "An automatic colon segmentation for 3d virtual colonoscopy," IEICE Transaction Information and Systems, E84-D(1):201-208, 2001.

[9] C.L. Wyatt, Y. Ge, D.J. Vining, "Automatic segmentation of the colon for virtual colonoscopy," Computerized Medical Imaging and Graphics, 24:1-9, 2000.

[10] Z. Liang, F. Yang, M. Wax, J. Li, J. You,A. Kaufman, L. Hong, H. Li, and A. Viswambharan, "Inclusion of a priori information in segmentation of colon lumen for 3d virtual colonoscopy," Conf. IEEE NSS-MIC, pages 1423-1427,1997.

[11] D. Chen, M.R. Wax, L. LI, Z. Liang, B. LI, and A.E. Kaufman, "A novel approach to extract colon lumen from ct images for virtual colonoscopy," IEEE Transactions on Medical Imaging, 19(12):1220-6, 2000.

[12] J.G. Fletcher, C.D. Johnson, W.R. Krueger, D.A. Ahlquist, H. Nelson, D. Il-strup, Harmsen, and E. Kay, "Corcoran1 Contrast-Enhanced CT Colonography in Recurrent Colorectal Carcinoma: Feasibility of Simultaneous Evaluation for Metastatic Disease, Local Recurrence, and Metachronous Neoplasia in Colorectal Carcinoma," American Journal of Roentgenology, 178:283-290, 2002.

[13] M.E. Zalis, J. Perumpillichira, and P.E. Hahn, "Digital Subtraction Bowel Cleansing for CT Colonography Using Morphological and Linear Filtration Methods," IEEE Transactions on Medical Imaging, 23(11), 2004.

[14] S. Lakare, M. Wan, M. Sato, A. Kaufman, "3D Digital Cleansing using Segmentation Rays," Proceedings of the conference on Visualization, 2000.

[15] R.M. Summers, M. Franaszek, M.T. Miller, P.J. Pickhardt., J.R.Choi, W.R. Schindler, "Computer-Aided Detection of Polyps on Oral ContrastEnhanced CT Colonography," American Journal of Roentgenology, 184:105-108, 2005.

[16] H. Li, P. Santago, "Automatic colon segmentation with dual scan CT colonography," Journal Digital Imaging, 18(1):42-54, 2005.

[17] Y. Masutani, H. Yoshida, P.M. MacEneaney, and A.H. Dachman, "Automated segmentation of colonic walls for computerized detection of polyps in ct colonography," Journal of Computer Assisted Tomography, 25(4):629-638, 2001.

[18] J. Napii, A.H. Dachman, P. Maceneaney, H. Yoshida, "Automated Knowledge Guided Segmentation of Colonic Walls for Computerized Detection of Polyps in CT Colonography," Journal of Computer Assisted Tomography, 26(4), 493-504, 2002.

[19] G. Iordanescu, J.P. Pickhardt, J.R. Choi, R.M. Summers, "Automated Seed Placement for Colon Segmentation in Computed Tomography Colonography," Academic Radiology, 12, 182-190, 2005.

[20] H. Frimmel, J. Nappi, and H. Yoshida, "Centerline-based colon segmentation for CT colonography," Medical Physics, 32:2665-2672, 2005.

[21] T.A. Chowdhury, P.F. Whelan, and O. Ghita, "A Method for Automatic Segmentation of Collapsed Colons at CT Colonography," Indian International Conference on Arti¯cial Intelligence (December) IICAI-05:3517- 3532, 2005.

[22] R.C. Gonzalez, R.E. Woods, Digital image processing, Reading MA: Addison Wesley, 1993.

[23] Atlas of Human Anatomy, Eagle Editions, ISBN: 1-902328-40-X.